

OPEN ACCESS

Sandwich Biobattery with Enzymatic Cathode and Zinc Anode Integrated with Sensor

To cite this article: D. Majdecka *et al* 2015 *J. Electrochem. Soc.* **162** F555

View the [article online](#) for updates and enhancements.

You may also like

- [High Performance Glucose/O₂ Biofuel Cell: Effect of Utilizing Purified Laccase with Anthracene-Modified Multi-Walled Carbon Nanotubes](#)
Michael Minson, Matthew T. Meredith, Alexander Shrier *et al.*
- [Study of Amperometric Response of Guaiacol Biosensor Using Multiwalled Carbon Nanotubes with Laccase Immobilized](#)
E. G. Uc-Cayetano, I. E. Villanueva-Mena, M. A. Estrella-Gutiérrez *et al.*
- [Investigating the Reversible Inhibition Model of Laccase by Hydrogen Peroxide for Bioelectrocatalytic Applications](#)
Ross D. Milton and Shelley D. Minteer



Your Lab in a Box!

The PAT-Tester-i-16: All you need for Battery Material Testing.

- ✓ All-in-One Solution with integrated Temperature Chamber!
- ✓ Cableless Connection for Battery Test Cells!
- ✓ Fully featured Multichannel Potentiostat / Galvanostat / EIS!

www.el-cell.com +49 40 79012-734 sales@el-cell.com

EL-CELL[®]
electrochemical test equipment





Sandwich Biobattery with Enzymatic Cathode and Zinc Anode Integrated with Sensor

D. Majdecka,^a S. Draminska,^a K. Stolarczyk,^a M. Kizling,^a P. Kryszynski,^a J. Golimowski,^a J. F. Biernat,^b and R. Bilewicz^{a,*}

^aDepartment of Chemistry, University of Warsaw, 02-093 Warsaw, Poland

^bDepartment of Chemistry, Gdansk University of Technology, 80-233 Gdansk, Poland

Carbon paper covered with side-naphthylated multi-walled carbon nanotubes was used as the conducting support for the construction of a biocathode in a hybrid biofuel cell (biobattery). Laccase *Cerrena unicolor* enzyme was employed as the catalyst for the 4e reduction of oxygen and a zinc disc covered with hopeite was used as the anode. Derivatized carbon nanotubes increase the working surface of the electrode and provide direct contact with the active sites of laccase. Biobattery characteristics under externally applied resistance, and power-time dependencies under flow cell conditions were evaluated. The system including the sandwich biobattery powering a dedicated two-electrode minipotentiostat with a simple sensor electrode was employed for monitoring a model neurotransmitter–catechol. The biobattery-powered sensor yielded the oxidation currents linearly dependent on catechol concentration in the range 0–2 mM and with a correlation coefficient of 0.998. This type of biobattery with laccase as the cathode catalyst can be integrated with analytical devices and power them even in long-time monitoring experiments.

© The Author(s) 2015. Published by ECS. This is an open access article distributed under the terms of the Creative Commons Attribution 4.0 License (CC BY, <http://creativecommons.org/licenses/by/4.0/>), which permits unrestricted reuse of the work in any medium, provided the original work is properly cited. [DOI: 10.1149/2.0731506jes] All rights reserved.

Manuscript submitted October 8, 2014; revised manuscript received March 3, 2015. Published March 11, 2015. This was Paper 989 presented at the Orlando, Florida, Meeting of the Society, May 11–15, 2014.

Biofuel cells (BFC) and hybrid biofuel cells (biobatteries) have several advantages over conventional fuel cells, e.g. they use enzymes—very efficient catalysts to transform chemical energy to electrical energy. The attractiveness of biofuel cells is due to possibilities of variety of applications of high energy density biofuels such as ethanol, glycerol and carbohydrates, work at room temperatures, at pH close to neutral and the products of reactions are environmentally-friendly.^{1–4} Enzymes are also less expensive than metallic catalysts used in conventional fuel cells and additionally are specific and selective, therefore do not require membrane separating electrode compartments. The biofuel cell can work as open-type device, and can be easily miniaturized.⁴ Initial market opportunities for biofuel cells are likely to be where there is a need for large amounts of energy but low power demands. This is because biofuel cells can achieve high efficiencies for oxidizing a given fuel, providing high energy density, but have lower power densities due to lower catalytic activity compared to metal catalyst based fuel cells.³ An important area of applications of the biofuel cells is powering electronic devices, e.g. clocks, timers or toys, small medical devices such as biosensors and drug delivery systems.^{5–9}

The number of enzyme molecules that can be directly bound to the conductive support is rather low, due to their large size leading to small surface concentration of catalytic active sites per electrode geometric area. Therefore application of a three dimensional conductive matrix is required. Carbon nanotubes increase the working surface area of the electrode and improve conductivity of the film. Furthermore, carbon nanotubes modified with different aryl groups provide easier access to the enzyme active sites and allow working in the direct electron transfer regime without any mediators.^{10–12}

Falk et al.⁹ demonstrated a wireless and self-powered biodevices composed of a wireless electronic unit, radio transmitter and self-sustained carbohydrate and oxygen biosensor powered by enzymatic fuel cell. Zhou and Wang⁷ reported biofuel cells for self-powered electrochemical biosensing and logic biosensing.

Narváez Villarrubia et al. used BFC based on carbon materials modified with bilirubin oxidase and glucose dehydrogenase bioanode for powering small devices.¹³ In a different approach, Lambert et al. proposed BFC with cellobiose dehydrogenase as bioanode catalyst and a bilirubin oxidase based biocathode,¹⁴ whereas Aquino Neto et al. proposed ethanol/oxygen hybrid biofuel cell composed of hybrid nanostructured bioanodes with immobilized alcohol dehydrogenase.¹⁵

Holade et al. reported a fuel cell to supply a pacemaker in human serum solution.¹⁶ BFC was proposed for interfacing biomolecular information processing and electronic system.¹⁷ The bioanode was based on PQQ-GDH and laccase was on the biocathode.

Biocomputing and bioanalytical applications of enzymatic system were described by Privman et al. who reported a biochemical threshold filtering mechanism.¹⁸

The BFC as a power supply in wireless sensor network (WSN) was reported by Gellett et al.³

Recently, we compared the efficiencies of a biofuel cell and biobattery. We developed a biofuel cell consisting of a biocathode covered with single-walled carbon nanotubes (SWCNTs) to connect laccase with the conducting support and bioanode covered with bioconjugates of SWCNTs with glucose oxidase and catalase. The biofuel cell gave power density of ca. 60 $\mu\text{W cm}^{-2}$ at 20 k Ω external resistance and open circuit potential was 0.5 V. Additionally we constructed a flow biobattery consisting of a GCE cathode covered with biphenylated SWCNTs, laccase and a zinc anode covered with a hopeite. The maximum power density was 0.6 mW cm^{-2} at 20 k Ω and the open circuit potential for biobattery was ca. 1.6 V. This biobattery showed a relatively high power and potential, hence, we thought it suitable for powering more demanding devices.⁸

In the present paper we employ the biobattery to power a handheld, custom-built minipotentiostat for controlling the potential of a catechol sensor, measuring the current and displaying it to the user. Catechol which is generated intensively in industrial processes, can be often found in the environment. Due to its reactivity and ability to accumulate in living organisms, the development of simple, efficient and quick analytical methods is vital for waste water analysis as well as medical applications.^{19–23} Moreover, catechol can be considered as a precursor of catecholamine-related neurotransmitters that are secreted in the brain by neurons and relay messages to the target cells. The optimal level of precursors and neurotransmitters, e.g. dopamine which originate from catechol plays a significant role in the functioning of the human body. Unsettled level of catecholamines causes neurological diseases such as Parkinson's disease or Schizophrenia. Therefore, the determination of catechol as the precursor of catecholamines involved in the brain-body integration is of importance in monitoring the attention span, learning, memory and variety of motivated behavior.^{24–26} Huang et al. described a sensor for catechol based on glassy carbon electrode modified with composite of silver nanoparticles, dopamine and graphene. They observed linear response in the catechol concentration range between 0.5 to 240 μM levels of catechol, and the limit of detection was 0.1 μM . The studies

*Electrochemical Society Active Member.

^zE-mail: bilewicz@chem.uw.edu.pl

showed enhanced catalytic efficiencies toward catechol oxidation.²⁴ Electrode materials for the electrochemical monitoring of catechol and dopamine were reviewed by Jackowska and Krysinski.²⁷ Njagy et al. developed a novel implantable enzyme-based carbon fiber biosensor which was fabricated by using tyrosinase immobilized on matrix composed of biopolymer, chitosan and ceria-based metal oxides deposited onto carbon fiber microelectrode.²⁸ Ahammad et al.²⁹ used glassy carbon electrode modified with poly(thionine) as a simple and sensitive electrochemical method for the detection of hydroquinone and catechol. Wang et al.³⁰ proposed a biosensor constructed by the electrodeposition of Au-clusters on poly (3-amino-5-mercapto-1,2,4-triazole) (p-TA) film on glassy carbon electrode used for dopamine, ascorbate, uric acid and nitrite detection.

The aim of our study was to integrate a biobattery as the source of power with a simple amperometric catechol sensor based on the oxidation of catechol on glassy carbon electrode by means of a custom-built, hand-held minipotentiostat to polarize a sensor electrode to the pre-determined potential and display the current being measured. The biobattery consists of a biocathode with laccase – the enzyme catalyzing 4-electron reduction of oxygen to water and adsorbed on naphthylated multi-walled carbon nanotubes (NAPH-MWCNTs) covering a carbon paper substrate (CP). Zinc disk covered with a layer of hopeite ($Zn/Zn_3(PO_4)_2$) served as the anode. The biobattery was employed under stationary or flow conditions.

Experimental

Materials and chemicals.— Catechol, potassium chloride (KCl), citric acid ($C_6H_8O_7$), disodium hydrogen phosphate (Na_2HPO_4), ethanol (C_2H_5OH) were purchased from POCh. Laccase *Cerrena unicolor* was obtained from the Department of Biochemistry (Maria Curie-Skłodowska University, Poland). Multi-walled carbon nanotubes (MWCNTs Cheap Tubes) were purchased from CheapTubes.com USA, Rue de la Vacherie, Belgium.

Modification procedures of the CNTs have been described elsewhere.⁵ Carbon paper (CP) was Toray Teflon Treated (TPG-H-030 Fuel Cell Store).

Laccase *Cerrena unicolor* C-139 was obtained from the culture collection of the Regensburg University and deposited in the fungal collection of the Department of Biochemistry (Maria Curie-Skłodowska University, Poland) under the strain number 139.^{31,32} Water was distilled and passed through Milli-Q purification system.

Thermogravimetric analyses (TGA) were done using Universal V4.3A TA Instrument. The measurements were carried out in argon atmosphere at a heating rate of 10 deg/min.

Electrochemical instrumentation and procedures.— The biobattery works under stationary or flow conditions. Carbon paper (CP) was modified with MWCNTs or naphthylated MWCNTs under reduced pressure. The modified and unmodified MWCNTs suspension was obtained by adding 8 mg nanotubes to 12 ml ethanol (4 ml of suspension for 3 CP electrodes). Electrode area was 3.14 cm^2 (Fig. 1A). Laccase (156 U/mg) was physically adsorbed on modified CP from 9 ml of McIlvaine buffer solution. After one day of laccase adsorption, the electrode was washed thoroughly with water and used as a biocathode in biobattery. In this arrangement, the zinc disk covered with zinc phosphate was used as the anode. Biobattery was composed



Figure 1. (A) Carbon Paper (CP) before and after modification, (B) Cathode contact in the biobattery (C) Construction of the biobattery designed for a flow system.

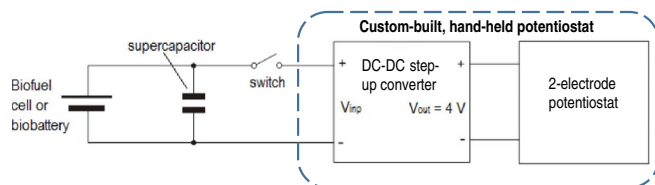


Figure 2. Scheme of circuitry composed of power source (biobattery with supercapacitor) and dedicated, custom-built minipotentiostat containing a DC-DC step-up converter which multiplies the initial potential of a single biobattery (V_{in}) to 4 V output potential (V_{out}), the latter supplies 2-electrode potentiostat electronics.

of three elements: cathode, anode and reaction compartment in between (Fig. 1C). Cathode contact of biobattery was made from glassy carbon material (Fig. 1B). McIlvaine buffer solution pH 5.3 as the suitable laccase environment was prepared by mixing of 0.1 M citric acid and 0.2 M disodium phosphate. Open circuit voltage (OCV) was measured in all experiments. Voltages between anode and cathode were measured under varying loads in the range from $10 \text{ M}\Omega$ to 1Ω . To minimize the power loss caused by dioxygen depletion during the testing of the cathode, measurements under each load were restricted to 5 seconds and were held under flow conditions.

Electrochemical experiments were performed using a hand-held minipotentiostat in a two-electrode configuration and, for comparison purposes, using a ECO Chemie Autolab Potentiostat in the same configuration. The hand-held minipotentiostat was custom-built by dr. S. Kalinowski (Warmia and Mazury University in Olsztyn, Department of Chemistry, Poland).

Fig. 2 shows the general scheme of such minipotentiostat. As it was supposed to be powered by a single biobattery (1.6 V), the minipotentiostat power supply part contains a DC-DC step-up converter, generating 4 V DC voltage required to power most of the electronics of this potentiostat, including the current measuring device, LCD display and potential control. This scheme in Fig. 2 contains also a supercapacitor permanently coupled in parallel to the biobattery as a power back-up, and a switch closing/opening the circuitry. In its “open” state it allows the biobattery to recharge itself and the supercapacitor between the measurements. When closed, both the biobattery and supercapacitor power the minipotentiostat for time span sufficient for amperometric detection of the analyte (catechol).

Chronoamperometric (CA) experiments for the catechol sensing were carried out in 0.1 M KCl aqueous supporting electrolyte using this minipotentiostat (or ECO Chemie Autolab as comparison) in a two electrode mode with glassy carbon (GC) electrode as working electrode of 0.008 cm^2 and silver chloride Ag/AgCl (KCl sat.) electrode as reference. The potential used for recording the CA oxidation current of catechol was set to +570 mV, hence 150 mV more positive than the voltammetric catechol oxidation peak.

Synthesis and characterization of modified MWCNTs.— 100 mg of pristine Multiwalled CNTs (CheapTubes) was placed in a round-bottom flask. To this flask 2.5 ml *o*-dichlorobenzene, 2.5 ml acetonitrile, 0.45 g 2-naphthylamine and 0.4 ml of amyl nitrite were added. The obtained mixture was sonicated for 5 h at 60–65°C. The reaction scheme is shown in Figure 3.

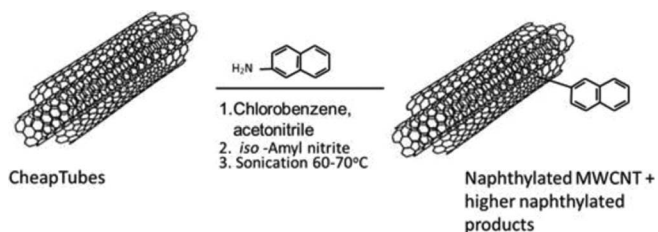


Figure 3. Scheme of synthesis of modified MWCNTs.

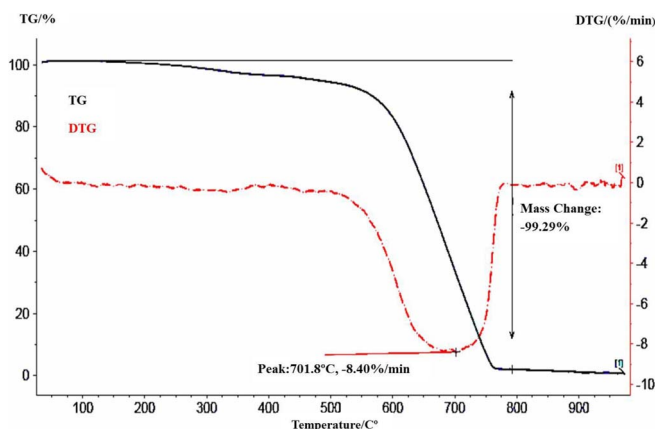


Figure 4. TGA of Naphthylated MWCNTs (CheapTubes).

Solid naphthylated MWCNTs were collected by filtration, then resuspended in dimethylformamide (DMF), sonicated briefly and centrifuged. This operation was repeated until the supernatant remained colorless. Then DMF was replaced by toluene and the purification procedure was repeated as above. Finally the solid material was washed with chloroform and dried under reduced pressure at 60°C.

The purification procedure yielded material in which wall-naphthylated component predominates.^{33,34} In our recent paper,³⁴ numerous CNTs derivatives prepared using reactions considered as occurring at the ends and/or on the walls of nanotubes were reviewed. Considerable differences of electrochemical properties suggested some excessive wall over end modifications of CNTs).

The naphthylation (functionalization) degree of MWCNTs was determined by thermogravimetric experiments. The results are shown in Fig. 4. The TGA for Cheap Tubes product below 200°C shows removal of only traces of solvents, so this mass decrease was not taken into account. The mass loss (16%; 16 mg, 0.125 mole) found in the range of 200–600°C corresponds to the removal of naphthyl residues. Considering the molecular mass of naphthalene (128) and carbon atomic mass, the modification degree equals ~0.018 moles of naphthalene residues per 1 mol of carbon atoms).

Results and Discussion

Electrochemical studies.— To check the activity of laccase, electrochemical experiments were performed. Figure 5 shows voltammograms for two different biocathodes. One of them was composed of

Table I. Catalytic current (mean value for 5 cathodes) measured at 0.2 V at electrodes covered with MWCNTs and MWCNTs modified with adsorbed laccase in deoxygenated (I_{bkg}) and saturated with dioxygen (I_{cat}) McIlvaine buffer solution (pH 5.3).

MWCNTs used for carbon paper modification*	I_{bkg} [μA]	I_{cat} [μA]	I_{cat} [μA] - I_{bkg} [μA]
MWCNTs	-35 ± 1.5	-97 ± 1	-62 ± 2
NAPH - MWCNTs	-83 ± 0.5	-254 ± 4	-171 ± 4.5

*Experiments were repeated 3 times.

carbon paper disk covered with unmodified multiwalled carbon nanotubes and adsorbed laccase (Fig. 5A) and the other (Fig. 5B) was made of CP covered with naphthylated MWCNTs and adsorbed laccase. The electrochemical experiments in the absence and presence of oxygen were performed. When the buffer solution was saturated with oxygen, catalytic curves of oxygen reduction for both biocathodes were observed which proved the activity of the adsorbed laccase. The catalytic waves of 4e direct reduction of oxygen to water appeared at the potential 0.6 V (vs. Ag, AgCl/1 M KCl_{aq} reference electrode). No mediators were needed. Naphthylated multiwalled carbon nanotubes give significantly larger currents of oxygen reduction than unmodified MWCNTs or naphthylated SWCNTs. Naphthyl groups are hydrophobic and possess conjugated double bonds. They are able to get closer to the hydrophobic pocket of the enzyme and provide more efficient direct electron transfer. For the cathode covered with naphthylated MWCNTs, the reduction current at 0.2 V was $-254 \mu\text{A}$ (Table I).

Flow biobattery.— After covering of the CP electrode with carbon nanotubes, laccase was adsorbed on the cathode and the biobattery with zinc anode was assembled. Zinc anode has a fixed highly negative and stable potential. We confirmed the stability of this potential inserting a reference electrode in the biobattery circuit, as shown in our recent work.⁸ It is, therefore, useful for testing various biocathodes and showing the influence of nanotubes modification on the current and power in biobatteries. Different external resistances were loaded to the circuit to evaluate the biodevice characteristics. Figure 6A allows to compare power-current dependencies for biobattery with cathodes based on CP covered with naphthylated and unmodified MWCNTs and adsorbed laccase *Cerrena unicolor* under flow conditions. Power plots obtained in the absence of enzyme and in argon saturated solution are also shown. Figure 6B presents the voltage-current dependencies for the same electrodes. The open circuit potential of the cell with

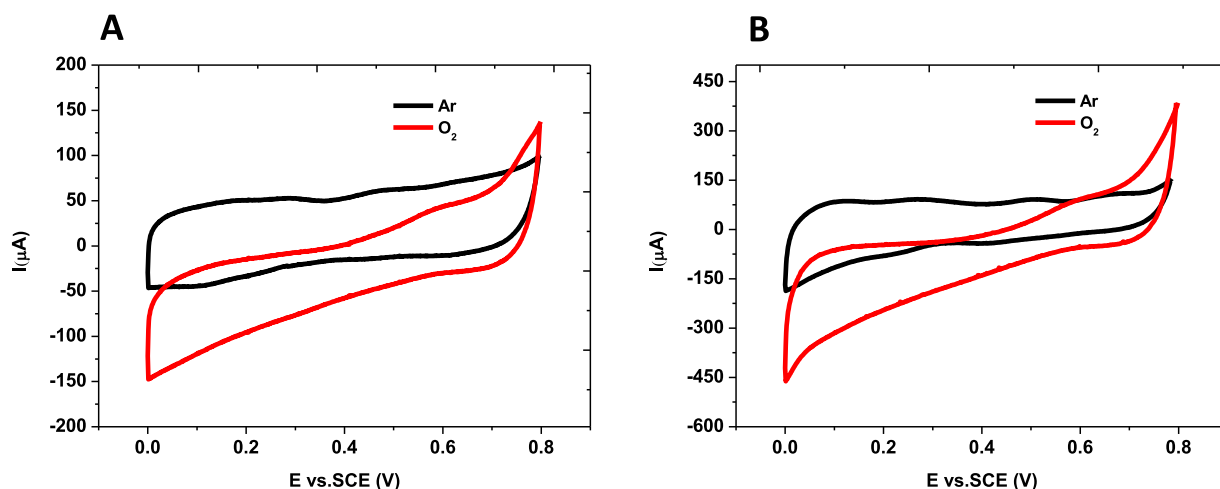


Figure 5. (A) Cyclic curves of carbon paper covered with MWCNTs and (B) modified naphthylated MWCNTs and adsorbed laccase. Experiments were conducted in oxygen (red line) or Ar (black line) in McIlvaine buffer solution (pH 5.3), scan rate was 5 mV s^{-1} .

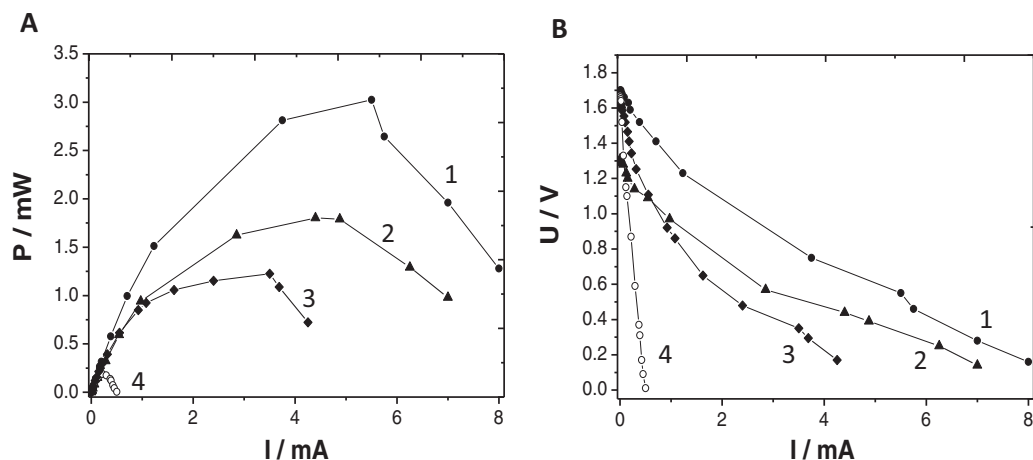


Figure 6. Power (A) and polarization (B) curves for the biobattery and battery under flow conditions in oxygen^{1,2,3} and Argon⁴ saturated 0.2 M McIlvaine buffer solution, pH 5.3. Cathode based on^{1,4} NAPH-MWCNTs and laccase,² NAPH-MWCNTs without laccase,³ MWCNTs with laccase.

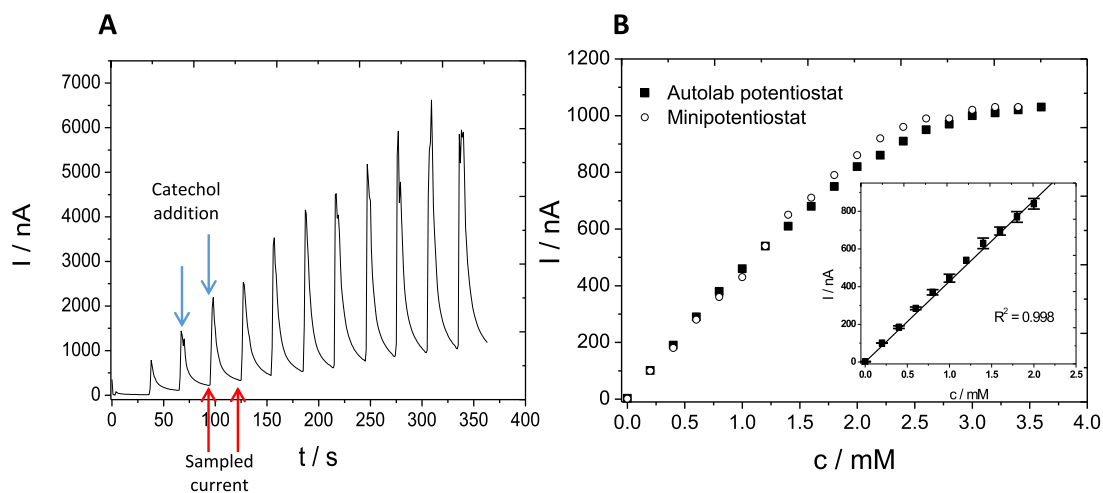


Figure 7. (A) I-t dependencies for the two-electrode sensor in 0.1 M KCl solution containing different catechol concentrations. GC electrode area: 0.008 cm². (B) Calibration curves for catechol in 0.1 M KCl solution obtained using (■) Autolab potentiostat and (○) hand-held minipotentiostat.

CP cathode covered with MWCNTs and laccase was 1.6 V and the maximum power was 1.2 ± 0.1 mW. The open circuit potential of the cell with CP cathode covered with NAPH-MWCNTs and laccase was 1.6 V and the maximum power was 3.1 ± 0.2 mW. The arylated nanotubes were shown to improve the performance of the cathode in the biobattery. Such powering unit is, therefore, promising as a source of energy for common sensing devices. For the three biobatteries connected in series, the open circuit potential was 5.1 V and power was 10 ± 1 mW, hence three times larger than those of the single cell without changes in the stability under working conditions (Fig. 1S).

Catechol sensor.— Chronoamperometry experiments were performed using either Potentiostat Autolab or our hand-held, custom-built minipotentiostat powered by the biobattery. Suitable constant potential of +570 mV (explained earlier) was selected. In Figure 7A the amperometric curves following each addition of 40 μ l of 100 mM solution of catechol are shown. Experiments were repeated five times. After each addition of catechol, the solution was vigorously stirred on magnetic stirrer before measurement (no stirring during the measurement).

The calibration curves for Potentiostat Autolab and minipotentiostat were almost the same and the correlation coefficient was at least 0.998 when current was probed 30 seconds after potential application (Fig. 7B.) The current was measured in concentration range from 0 to 3.5 mM of catechol and showed linearity in the range from 0 to 2 mM.

The relative standard deviation of the biosensor response to 2 mM catechol was 9% for 3 measurements. The system consisting of a single sandwich biobattery (shown in Fig. 8) was used for powering the sensor and generating data shown in Fig. 7.

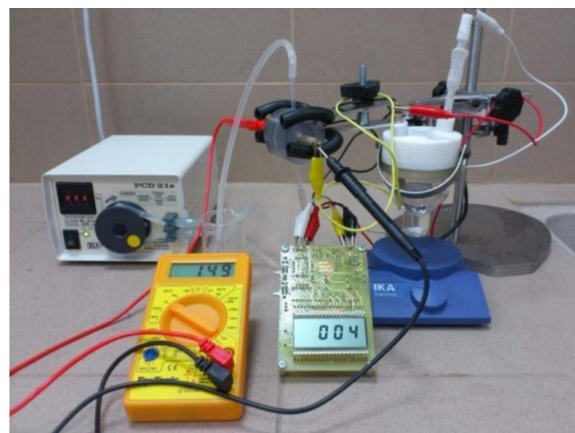


Figure 8. Enzymatic biobattery integrated with minipotentiostat and biosensor.

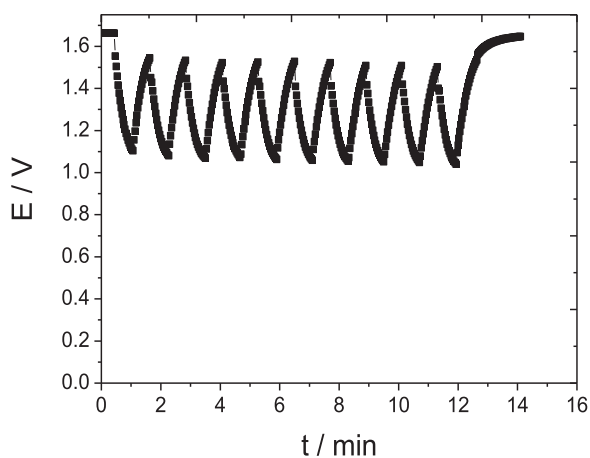


Figure 9. Potential-time dependence of a single biobattery with supercapacitor, powering the minipotentiostat (as a load) being switched on and off every 60 s – a time span sufficient for sensor readout.

Enzymatic biobattery powering the sensing unit.— In Figure 9 the potential-time dependence for a single cell biobattery powering the minipotentiostat is shown. The integrated system was switched on and off every 60 seconds, a time sufficient to make the readout of the current measured. Following the discharging of the biobattery, the potential is regenerated in 60s to 1.55 V and after 120s it achieves the initial value equal to the open circuit potential.

Conclusions

The biobattery with $\text{Zn}/\text{Zn}_3(\text{PO}_4)_2$ anode was constructed and two nanostructured electrodes were tested as the biocathodes. The cathode composed of carbon paper covered with covalently naphthylated MWCNTs and laccase allowed to obtain significantly higher power densities compared to a similar cathode but with unmodified MWCNTs. We ascribe it to improved electrical connection between the electrode and the active centers of laccase. The naphthylated residues connected to MWCNTs seem to be crucial for the efficiency of direct electron transfer to the enzyme molecules so that no mediators are needed. The parameters of the biobatteries: power and open circuit potential were evaluated. The power of the biobattery with naphthylated MWCNTs on the cathode exceeded 3.1 ± 0.2 mW. The open circuit potential measured for all systems containing arylated MWCNTs and unmodified MWCNTs on CP substrate and adsorbed laccase was ca. 1.6 V.

The system including biobattery, a home-made minipotentiostat and a small GC electrode based neurotransmitter sensor was tested in the chronoamperometric determination of 0 to 2 mM catechol. The single cell biobattery is suitable for powering small sensing devices and does not need mediators for on the biocathode side. Slow oxidation of Zn anode is not favorable if the device is designed for using in the living organism; however, the open circuit potentials for such a hybrid cell are more than twice as large as the values obtained for the best of full biofuel cells reported so far (with enzymatic both cathode and anode) The biobattery is, therefore, currently a reasonable solution as an external powering unit and work on the improvement of the full biofuel cell is continued in our laboratory.

Several aspects of device must be refined in further research. Most important, is finding an efficient enzymatic anode to avoid using Zn. Fructose dehydrogenase is an example of enzyme working at the anode in a mediatorless regime as we demonstrated in a recent communication.³⁵ At present, the system lifetime, shorter than that of common batteries, is limited primarily by the inability of the enzymes to regenerate sufficiently fast. Additionally, the enzymes are prone to denaturation under constant load conditions. Our device, therefore, is designed to work under pulsed conditions. The amount of modifying material and its real surface can be made larger e.g. by

pressing MWCNT with enzyme, as demonstrated by Agnes et al.³⁶ Where needed, the charge pump and DC-DC converter can be used to adjust the voltage to values required by the powered device as shown by Katz et al.^{16,37} Moreover, the cost of materials used in series production (carbon nanotubes, enzyme) is still decreasing, therefore this direction for powering small devices is really promising.

Acknowledgments

This work was supported by grant PSPB 079/2010 from Switzerland through the Swiss Contribution to the enlarged European Union. We thank dr. Slawomir Kalinowski for the construction of the minipotentiostat.

References

1. S. C. Barton, J. Gallaway, and P. Atanassov, *Chem. Rev.* **104**, 4867 (2004).
2. J. A. Cracknell, K. A. Vincent, and F. A. Armstrong, *Chem. Rev.* **108**, 2439 (2008).
3. W. Gellert, M. Kesmez, J. Schumacher, N. Akers, and S. D. Minter, *Electroanalysis*, **22**, 727 (2010).
4. A. Heller, *Phys. Chem. Chem. Phys.* **6**, 209 (2004).
5. P. Cinquin, Ch. Gondran, F. Giroud, S. Mazabrard, A. Pellissier, F. Boucher, J. P. Alcaraz, K. Gorgy, F. Lenouvel, S. Mathe, P. Porcu, and S. Cosnier, *PLoS ONE* **5**, e10476 (2010).
6. U. B. Jensen, S. Lörcher, M. Vagin, J. Chevallier, S. Shipovskov, O. Korelova, F. Besenbacher, and E. E. Ferapontova *Electrochim. Acta* **62**, 218 (2012).
7. M. Zhou and J. Wang, *Electroanalysis*, **24**, 197 (2012).
8. K. Stolarczyk, M. Kizling, D. Majdecka, K. Żelechowska, J. F. Biernat, J. Rogalski, and R. Bilewicz, *J. Power Sources* **249**, 263 (2014).
9. M. Falk, M. Alcalde, P. N. Bartlett, A. L. De Lacey, L. Gorton, C. Gutierrez-Sanchez, R. Haddad, J. Kilburn, D. Leech, R. Ludwig, E. Magner, D. M. Mate, P. Ó. Conghaile, R. Ortiz, M. Pita, S. Pöller, T. Ruzgas, U. Salaj-Kosla, W. Schuhmann, F. Sebelius, M. Shao, L. Stoica, C. Sygmund, J. Tilly, M. D. Toscano, J. Vivekananthan, E. Wright, and S. Shleev, *PLoS ONE*, **10**, 9 (2014).
10. K. Stolarczyk, D. Łyp, K. Żelechowska, J. F. Biernat, J. Rogalski, and R. Bilewicz, *Electrochim. Acta* **79**, 74 (2012).
11. K. Stolarczyk, M. Sepełowska, D. Łyp, K. Żelechowska, J. F. Biernat, J. Rogalski, K. D. Farmer, K. N. Roberts, and R. Bilewicz, *Bioelectrochem.* **87**, 154 (2012).
12. M. Karaškiewicz, D. Majdecka, A. Więckowska, J. F. Biernat, J. Rogalski, and R. Bilewicz, *Electrochim. Acta* **126**, 132 (2014).
13. C. W. Narváez Villarrubia, C. Lau, G. P. M. K. Ciniciato, S. O. Garcia, S. S. Sibbett, D. N. Petsev, S. Babanova, G. Gupta, and P. Atanassov, *Electrochem. Commun.* **45**, 44 (2014).
14. P. Lamberg, S. Shleev, R. Ludwig, T. Arnebrant, and T. Ruzgas, *Biosens. Bioelectron.* **55**, 168 (2014).
15. S. Aquino Neto, T. S. Almeida, L. M. Palma, S. D. Minter, and A. R. de Andrade, *J. Power Sources*, **259**, 25 (2014).
16. Y. Holade, K. MacVittie, T. Conlon, N. Guz, K. Servat, T. W. Napporn, K. B. Kokoh, and E. Katz, *Electroanalysis*, **26**, 2445 (2014).
17. K. MacVittie and E. Katz, *Chem. Commun.* **50**, 4816 (2014).
18. V. Privman, S. Domanskyi, S. Mailloux, Y. Holade, and E. Katz, *J. Phys. Chem.* **118**, 12435 (2014).
19. C. T. Jung, R. R. Wickett, P. B. Desai, and R. L. Bronaugh, *Food Chem. Toxicol.* **41**, 885 (2003).
20. S. R. Nambiar, P. K. Aneesh, and T. P. Rao, *Analyst* **138**, 5031 (2013).
21. M. Portaccio, S. Di Martino, P. Maiuri, D. Durante, P. De Luca, M. Lepore, U. Bencivenga, S. Rossi, A. De Maio, and D. G. Mita, *J. Mol. Cat. B: Enzymatic* **41**, 97 (2006).
22. X. Wang, Q. Cao, L. Liang, J. Chen, C. You, Y. Ruan, H. Lin, and L. Wu, *Talanta*, **117**, 359 (2013).
23. S. Lupu, C. Lete, M. Marin, and N. Totir, *Electrochim. Acta* **54**, 1932 (2009).
24. K.-J. Huang, L. Wang, J. Li, M. Yu, and Y.-M. Liu, *Microchem. Acta* **180**, 751 (2013).
25. A. Galvan and T. Wichmann, *Clin. Neurophysiol.*, **119**, 1459 (2008).
26. J. W. Dalley and J. P. Roiser, *NeuroScience*, **215**, 42 (2012).
27. K. Jackowska and P. Krysiński, *Anal. Bioanal. Chem* **405**, 3753 (2013).
28. J. Njagi, M. M. Chernov, J. C. Leiter, and S. Andreescu, *Anal. Chem.* **82**, 989 (2010).
29. A. J. S. Ahammad, Md. M. Rahman, G.-R. Xu, S. Kim, and J.-J. Lee, *Electrochim. Acta* **56**, 5266 (2011).
30. C. Wang, R. Yuan, Y. Chai, Y. Zhang, F. Hu, and M. Zhang, *Biosens. Bioelectron.* **30**, 315 (2011).
31. J. Rogalski, M. Wojtas-Wasilewska, R. Apalovič, and A. Leonowicz, *Biotechnol. Bioeng.* **37**, 770 (1991).
32. J. Rogalski and G. Janusz, *Prep. Biochem. Biotechnol.* **40**, 242 (2010).
33. A. Hirsch, *Angew. Chem. Int. Ed.* **41**, 1853 (2002).
34. K. Żelechowska, K. Stolarczyk, D. Łyp, J. Rogalski, K. P. Roberts, R. Bilewicz, and J. F. Biernat, *Biocybernetics and Biomedical Engineering* **33**, 235 (2013).
35. M. Kizling, K. Stolarczyk, J. Sim Sin Kiat, P. Tammela, Z. Wang, L. Nyholm, and R. Bilewicz, *Electrochem. Commun.* **50**, 55 (2014).
36. Agnes M. Holzinger, A. Le Goff, B. Reuillard, K. Elouarzaki, and S. Tingry, *Energy Environ. Sci.* **7**, 1884 (2014).
37. M. Southcott, K. MacVittie, J. Halamek, L. Halamkova, W. D. Jemison, R. Lobeld, and E. Katz, *Phys. Chem. Chem. Phys.* **15**, 6278 (2013).